2014

Numerical Analysis of Suction Mufflers

Joaquim Rigola
Heat and Mass Transfer Technological Center – Universitat Politècnica de Catalunya, Terrassa (Barcelona), Spain, quim@cttc.upc.edu

Joan López
Heat and Mass Transfer Technological Center – Universitat Politècnica de Catalunya, Terrassa (Barcelona), Spain, joanl@cttc.upc.edu

Giorgos Papakokkinos
Heat and Mass Transfer Technological Center – Universitat Politècnica de Catalunya, Terrassa (Barcelona), Spain, giorgos@cttc.upc.edu

Oriol Lehmkuhl
Termo Fluids S.L., Sabadell (Barcelona), Spain, oriol@cttc.upc.edu

Assensi Oliva
Heat and Mass Transfer Technological Center – Universitat Politècnica de Catalunya, Terrassa (Barcelona), Spain, oliva@cttc.upc.edu

Numerical Analysis of Suction Mufflers

Joaquim RIGOLA[1*], Joan LÓPEZ[1], Giorgos PAPAKOKKINOS[1],
Oriol LEHMKUHL[1,2], Assensi OLIVA[1]

[1]Heat and Mass Transfer Technological Center (CTTC)
Universitat Politècnica de Catalunya – Barcelona TECH (UPC),
Colom, 11, E-08222, Terrassa (Barcelona), Spain
Tel. +34 93 739 81 92
Email: cttc@cttc.upc.edu, http://www.cttc.upc.edu

[2]Termo Fluids S.L.
Magí Colet, 8, E-08204 Sabadell (Barcelona), Spain
Tel. +34 93 783 61 13
Email: termofluids@termofluids.com , http://www.termofluids.com

* Corresponding author

ABSTRACT

The aim of this paper is to present the numerical resolution of suction muffler configurations (by means of a tridimensional, unstructured, parallel and object oriented CFD&HT TermoFluids code (Lehmkuhl, *et al*. 2007) specially adapted to low Mach models (Lopez *et al.* 2012), coupled with the numerical resolution of the whole compressor domain (by means of a modular, unstructured and object oriented NEST-compressors tool (Damle *et al.* 2011) to simulate the thermal and fluid dynamic behavior of hermetic reciprocating compressors).

The numerical results aim to evaluate the influence of the suction muffler geometry on the mass flow rate and compressor efficiency performance, while considering the whole compressor working conditions in a coupling manner. In that sense, the CFD&HT resolution of the muffler is obtained with boundary conditions obtained from the numerical simulation of the rest of the hermetic reciprocating compressor.

The use of Large Eddy Simulation (LES) models for the turbulent suction muffler analysis; the adaptation of Low Mach formulation avoiding the full incompressible numerical problem, and the coupling of a numerical simulation model of the whole compressor as boundary conditions, are the important updated numerical aspects presented in this paper.

1. INTRODUCTION

One of the most important aspects of compressor design and efficiency improvement is to fully understand the thermal and fluid dynamic behavior of the fluid flow. In that sense suction muffler plays an important role, where pressure pulsation reduction through it to avoid noise has a significant influence on compressor performance reduction. Thus, suction muffler design has to be a compromise between the better performances with a low noise level.

(Singh and Soedel, 1974) presented a numerical model for the analysis of pulsating flows oriented to muffler design, mainly based on one dimensional acoustic wave equation through each one of compressor components. In a similar manner, (Pérez-Segarra, et al. 1994) presented a numerical simulation model of the thermal and fluid dynamic behavior of hermetic reciprocating compressors based in the transient and one-dimensional resolution of the conservation equations of mass, momentum and energy under a fully implicit and compressible formulation, allowing not only the performance efficiency analysis of the compressor but also the pressure pulsations and transmission losses generated.

On the other hand, (Choi et al. 2000) presented the first CFD analysis of suction muffler behavior based on Navier Stokes equations resolution by means of finite volume techniques. In this case, suction muffler is analyzed as an independent element with constant boundary conditions. (Nakano et al. 2008) presented the first CFD analysis of suction muffler behavior using as a pressure boundary condition the once obtained from a numerical simulation of the whole compressor based on one-dimensional acoustic wave (Singh et al. 1974). (Pereira et al. 2008) do the same although using as a boundary condition experimental compression chamber pressure distribution experimentally obtained. Finally, (Sarioglu et al. 2012) presented a wide range of numerical cases using these last numerical scheme usually used.

The present paper is focused on: the CFD&HT numerical resolution using 3D unstructured, parallel and object code that mainly uses Large Eddy Simulation (LES) turbulence models, instead of the classical Reynolds Average Navier-Stokes equations, where compression chamber pressure is numerically obtained from a one dimensional transient and fully compressible formulation code. A first numerical illustrative analysis of two different geometries has been carried to show the possibilities that this kind of tools can offer.

2. CFD&HT NUMERICAL MODEL

The 3D numerical analysis of suction muffler is based on a multi-dimensional explicit finite volume fractional-step based algorithm extended to simulate low Mach fluxes using a Runge-Kutta/Crank-Nicholson time integration scheme, with a symmetry preserving discretization. Turbulence modeling is an extension of the WALE (Wall Adapting Local Eddy-viscosity) (Nicoud, F. and Ducros, F., 1999) model applied to non-structured meshes. The pressure equation is solved by means of direct Schur decomposition solver for coarse meshes, while the iterative CG Diagonal is the one used for fine meshes.

2.1 Navier-Stokes equations resolution

A general view of the most important details about Navier-Stokes equations discretization, extended to low Mach number compressible flow –giving incompressible hypothesis as a particular case- and the Large Eddy Simulation model used are here presented. The numerical model presented has been used from a general CFD&HT framework TermoFluids code (Lehmkuhl, et al. 2007) and the last updates regarding low Mach formulation (Chiva et al. 2011).

The Low Mach number approximation of the Navier-Stokes equations is obtained by expanding the variables of the compressible equations into power series of the Mach number and keeping the lower order terms, thus obtaining

$$\Omega_c \frac{d\rho_c}{dt} + Mu_c = 0_c \tag{1}$$

$$\Omega_c \frac{d(\rho_c u_c)}{dt} + C(\rho_c u_c)u_c + Du_c + \Omega_c G p_{d,c} = 0_c \tag{2}$$

$$\Omega_c \frac{d(\rho_c h_{s,c})}{dt} + C(\rho_c u_c)h_{s,c} + DT_c + \tau : Gu_c = 0_c \tag{3}$$

where u_c and $\tau \in \Re^m$ are the velocity vector and the viscous stress tensor, while h_s, p_d, $\rho_c \in \Re^q$ are enthalpy, hydrodynamic part of the pressure, and fluid density.

The matrices C and $D \in \Re^{m \times m}$ are the convective and diffusive operators, respectively. Note the u-dependence of the convective operator (non-linear operator). Finally, $G \in \Re^{m \times q}$ represents the gradient operator, while $M \in \Re^{q \times m}$ the matrix is the divergence operator.

The substance being modeled is assumed to follow the ideal gas law

$$p_o = \rho RT \tag{4}$$

where p_o is the thermodynamic part of the pressure and is assumed constant.

2.2 Global Numerical resolution

The global numerical resolution is mainly based on a variant of the Predictor-Corrector scheme shown by (Najm et al. 1998) (Nicoud, F. 2000) to solve the set of equations (3)-(6). Computing an initial estimated density and temperature map, the pressure-velocity coupling is solved by a fractional step as described by (Lehmkuhl, O. et al.

2007) obtaining a first estimated predictor velocity field. With the velocity field obtained, an updated density and temperature map is evaluated by means of state and energy equations. Finally, a second fractional step is solved to obtain the next time-step velocity field. Present resolution keeps incompressible fractional step resolution as a particular case (Rigola et al. 2012).

Scalar transport terms discretization involves a second order backward difference scheme for the temporal term, and an Adams-Bashforth for the other terms at the predictor-step and a Crank-Nicholson scheme at the corrector-step.

2.3 Fractional step solving

For the temporal discretization of the momentum equation (4), a second order backward difference scheme is used for the time derivative term, a fully explicit second-order one-leg scheme (Verstappen, R. and Velman, A., 2003) for the right-hand-side terms of the momentum equation except the pressure gradient $\left(R(u_c) := \Omega^{-1}\left(-C\left(\rho_c u_c\right)u_c - D\rho_c u_c\right)\right)$ and a first-order backward Euler scheme for the pressure gradient.

$$\Omega_c \frac{d\rho_c}{dt} + Mu_c^{n+1} = 0_c \tag{5}$$

$$\frac{(\beta+1/2)\rho'_c u_c^{n+1} - 2\beta\rho_c^n u_c^n + (\beta-1/2)\rho_c^{n-1}u_c^{n-1}}{\Delta t} = R((1+\beta)\rho_c^n u_c^n - \beta\rho_c^{n-1}u_c^{n-1}) - G_c p_c^{n+1} \tag{6}$$

where the parameter β is computed each time-step to adapt the linear stability domain of the time integration scheme to the instantaneous flow conditions in order to use the maximum Δt possible, under incompressible hypothesis.

The unstructured spatial discretization schemes are conservative, that is, they preserve the kinetic energy equation, and doing so, it is possible to assure good stability properties even at high Reynolds numbers with coarse meshes. It is held if and only if the discrete convective operator is skew symmetric $\left(C_c(u_c) = -C_c^*(u_c)\right)$ and if the negative conjugate transpose of the discrete gradient operator is exactly equal to the divergence operator $\left(-(\Omega_c G_c)^* = -M_c\right)$. Since the diffusive terms must be strictly dissipative $\left(u_c^*(D_c + D_c^*)u_c \geq 0\right)$ the diffusive operator D_c must be symmetric and strictly-definitive.

Under these conditions the velocity-pressure coupling is solved twice, both by means of the classical fractional step projection method (Yaneko, N.N., 1971).

$$u_c^p = u'_c + G\tilde{p}_c / \rho'_c \tag{7}$$

where the pseudo-pressure is $\tilde{p}_c = \tilde{p}_c^{n+1}\Delta t/(\beta+1/2)$ and u_c^p is the predicted velocity. The discrete Poisson equation for $\tilde{p}_c$ is obtained by taking the divergence of equation (9) and after applying the continuity equation

$$Lp_c = M\rho'_c u_p^c + \Omega_c \partial\rho_c / \partial t \tag{8}$$

where the discrete Laplacian operator $L \in \Re^{q\times q}$, is by construction, a symmetric positive definite matrix $L \equiv M\Omega_c^{-1}M^*$. Once the solution is obtained, u'_c results from the correction: $u_c^{'} = u_c^p - G\tilde{p}_c / \rho'_c$.

In an iterative manner, energy equation and gas law equation updates temperature $T_c^{n+1} = T_c^{'}$ and density $\rho_c^{n+1} = \rho_c^{'}$ maps, which allows obtaining a final $u_c^{n+1} = u'_c$ velocity field.

It is very important to highlight that this numerical algorithm resolution applied for low Mach conditions, gives incompressible hypothesis as a particular case where $T_c^{'} \equiv T_c^{n+1}$ and $u'_c \equiv u_c^{n+1}$ in the one step algorithm.

2.4 Turbulence modelling

In the quest for a correct modelling of Navier Stokes equations, they can be filtered spatially like in Large Eddy Simulation (LES). Restricting ourselves to the non-equilibrium fixed-parameter SGS model from (Yoshizawa et al. 2000), the filtered non-linear convective term must be modeled as,

$$\rho\frac{\partial\overline{u}_c}{\partial t}+\mathrm{C}(\overline{u}_c)\overline{u}_c+\mathrm{D}\overline{u}_c+\mathrm{G}\overline{p}_c=\mathrm{C}(\overline{u}_c)\overline{u}_c-\overline{\mathrm{C}(u_c)u}_c\approx-\frac{\partial\tau_{ij}}{\partial x_j} \tag{9}$$

where the filtered velocity is denoted by $\overline{u}_c$ and the SGS stress (τ_{ij}) is defined as, $-2\nu_S\overline{S}_{ij}+\frac{1}{3}\tau_{ij}\delta_{ij}$. Now is only necessary to define a suitable expression for the SGS viscosity.

The last model implemented in TermoFluids code, has been the wall-adapting eddy viscosity model (WALE) proposed by (Nicaud and Ducros 1999). This model is based on the square of the velocity gradient tensor. In its formulation the SGS viscosity accounts for the effects of both, the strain and the rotation rate of the smallest resolved turbulent fluctuations. In addition, the proportionality of the eddy viscosity near walls is recovered without any dynamic procedure,

$$\nu_{sgs}=(C_w\Delta)^2\frac{(\nu'_{ij}:\nu'_{ij})^{3/2}}{(S'_{ij}:S'_{ij})^{5/2}+(\nu'_{ij}:\nu'_{ij})^{5/4}} \tag{10}$$

$$S'_{ij}=\frac{1}{2}\left[G(\overline{u'_c})+G*(\overline{u'_c})\right] \tag{11}$$

$$\nu'_{ij}=\frac{1}{2}\left[G(\overline{u'_c})^2+G*(\overline{u'_c})^2\right]-\frac{1}{3}\left(G(\overline{u'_c})^2 I\right) \tag{12}$$

3. HERMETIC RECIPROCATING COMRPESSORS NUMERICAL MODEL

The simulation of a reciprocating compressor is addressed considering it as a thermal and fluid-dynamic system. This allows employing a parallel partitioned coupled approach: several components conforming the compressor-system are identified and modeled separately. By coupling these models any compressor configuration can be simulated. The simulation is done by using an in-house object oriented parallel code framework for simulation of multiphysics and multiscale systems. As stated by its name, this code is a generalist software solution to simulate problems involving mixed phenomena, commonly found in many engineering and science applications.

The resolution algorithm of this code is based on a partitioned coupled approach. This provides an efficient way to simulate physical systems in a modular way. Unlike monolithic approaches, partitioned strategies allow rapid setup of the simulated cases which is very useful when new system configurations must be tested.

3.1 Compressor component models

Viewed as a thermal and fluid dynamic system, a reciprocating compressor is composed on several elements such as tubes, chambers, valves, compression chambers and so on (see Fig. 1). Each element has some physical entity representing one or several phenomena (fluid flow, heat transfer, etc.) occurring inside its domain.

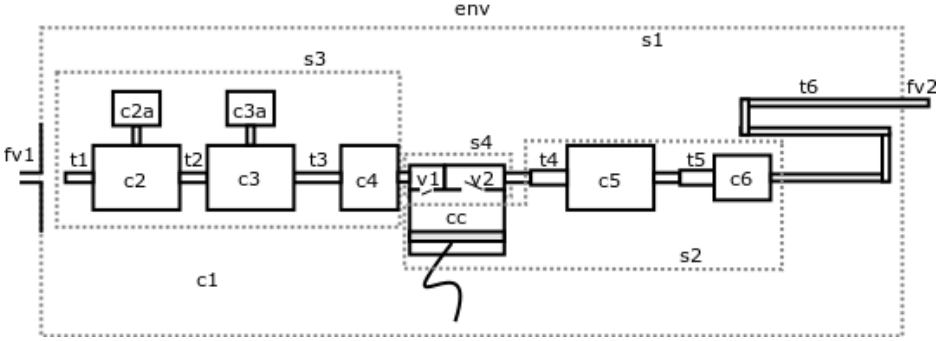

Figure 1. Example scheme of a compressor configuration.

The employed partitioned approach assumes that each element composing the compressor system must be able to solve itself by giving the appropriate boundary conditions. Therefore each component must be assigned with a specific computational model. Such a model can be queried in order to know the state of the element and/or update the boundary conditions of its surrounding elements (see Fig. 2).

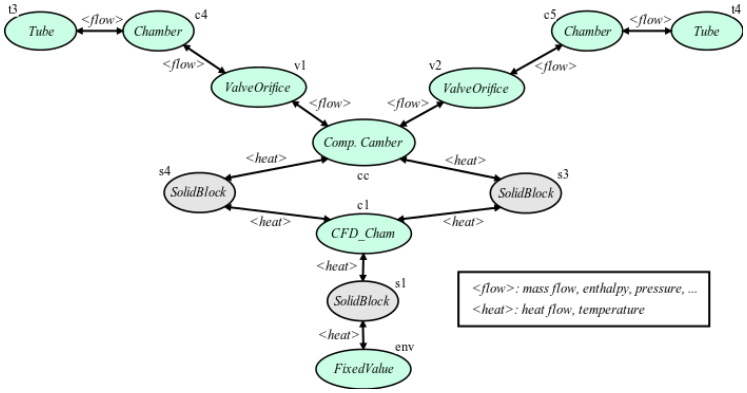

Figure 2. The compressor as a set of elements exchanging *flow* and/or *heat* information between each other.

The phenomena taking place inside the elements that compose a reciprocating compressor are resolved by means of the computational models from Table 1.

Table 1. Available families of computational models.

Tube	Pressure-based methods SIMPLEC algorithm using staggered mesh for velocity map. Upwind criteria are used for convective terms.
Chamber	Pressure correction approach (in the same way as Tube)
ValveOrifice	Multidimensional model based in modal analysis. Valve position is obtained by means of an iterative method.
CFD_Cham	Low-Mach based CFD&HT model for compressible flow available to be used in every part of the compressor.
SolidBlock	Based on a global balances considering heat exchange with fluid, environment and surrounding solid parts.
Solid1D	Similar as SolidBlock, but uses 1D discretization.
FixedValue	It is a simple built-in type to fix boundary conditions.

The mathematical formulation of these models is detailed in (Pérez-Segarra et al 2003, Damle et al. 2008). For details in the CFD&HT models one must refer to (Lehmkuhl 2007, Lehmkhul 2012, Borrell 2012). In Table 2 different zones from the compressor configuration in Figures 2 and 3 are associated with the models used to their resolution.

4. COMPUTATIONAL DOMAIN, MESH AND BOUNDARY CONDITIONS

Figure 3 shows both different muffler geometries that have been considered for comparison purposes. Figure 3a shows a two chambers muffler where flow mainly fills all first chamber, while Figure 3b shows a two chamber muffler where fluid flow goes mainly directly from the entrance to the second suction chamber muffler. Academic configurations are presented to show the influence of direct vs. indirect flow from compressor inlet to suction valve. First chamber height is 2.7 times second chamber height; while width of both chambers is the double of the thickness.

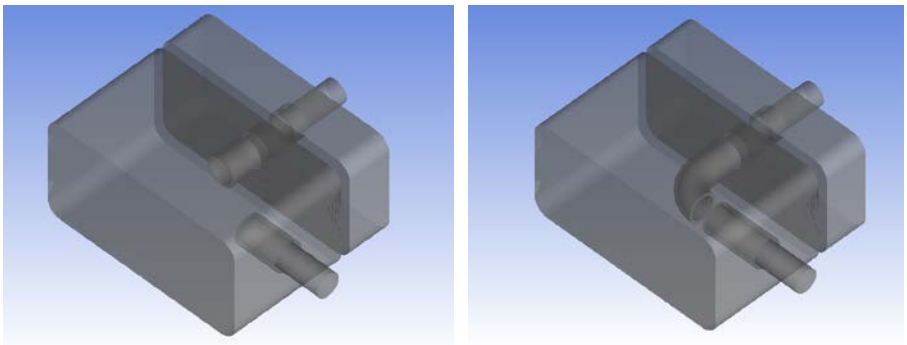

Figure 3. Muffler geometry (a) indirect (b) direct fluid flow from first chamber to second chamber.

Both configurations present a mesh depicted in Figure 4. The mesh consists of tetrahedral cells exclusively. During the meshing process, special attention has been given in the regions where steep gradients are present (jet path, tubes interior etc.), while a coarser mesh is used in regions where the flow is dictated mainly by natural convection. Indicatively, the average density of the meshes under consideration ranges between 5 and 10 cells/cm^3 approximately.

Dirichlet (no-slip) condition is imposed for the velocity at all the walls of the muffler. At the inlet, the velocity has a uniform fixed value. The temperature boundary condition is Dirichlet at the inlet and the walls, while at the outlet the temperature boundary condition is Neumann. The pressure at the outlet is provided in terms of two values – the static pressure after the outlet (p_∞) and the expansion coefficient at the outlet (γ).

The exact values of the boundary conditions arise from the numerical interaction of the muffler with the other compressor elements.

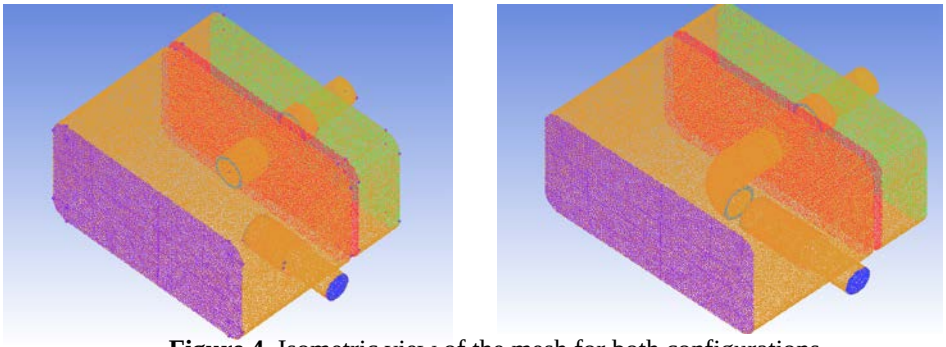

Figure 4. Isometric view of the mesh for both configurations.

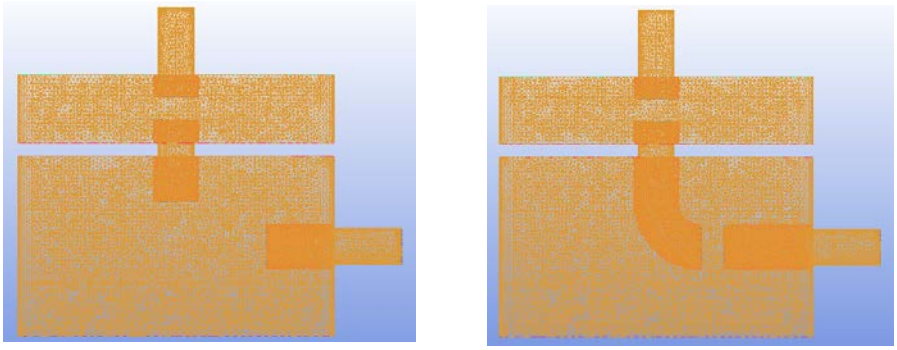

Figure 5. Front view of the mesh for both configurations.

4.1 Verification procedure

In the present paper verification results presented are based on the analysis of mesh density depending on the number of CV. Different papers oriented for example, on valve analysis (Rigola et al. 2012), or circulated fluid flow through shell (Lopez et al. 2012) have previously presented analysis of SGS eddy viscosity models.

The mesh independence study pertains to the simulation of a steady state case (all boundary conditions have fixed values). The expected result of such simulation is that the influence of the initial condition is eliminated and the solution converges to the steady state solution. The mesh independence analysis is depicted in Figure 6. It shows a non-dimensional pressure drop as a function of time, for 4 different meshes (675000 CVs; 800000 CVs; 1000000 CVs and 1200000 CVs).
Table 2 also shows the non-dimensional pressure drop (pressure drop along suction muffler divided by inlet dynamic pressure) taken as the average value of the last 1000 iterations, in order to smooth out the fluctuations. It is clear that all of them converge to the steady state solution, while differences between smoothest meshes are around 0.26%, while differences on finest meshes are around 0.12%.

Table 2. Non-dimensional pressure drop convergence analysis.

Mesh size	675k	800k	1000k	1200k
Pressure drop	2.0355	2.0409	2.0390	2.0379

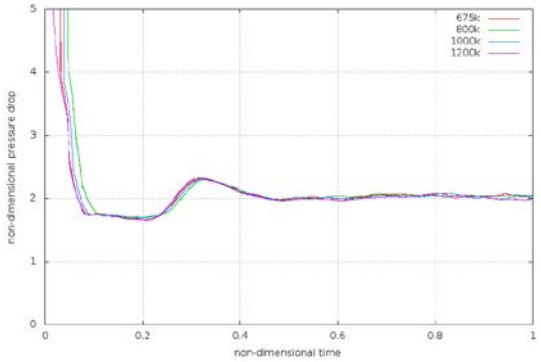

Figure 6 Non-dimensional pressure drop evolution.

5. NUMERICAL RESULTS

Two different numerical illustrative results are here presented for both (A) and (B) suction muffler configurations presented above. The aim of these numerical results is to show the influence of pressure drop on both configurations, for an inlet mass flow rate and an outlet muffler pressure obtained from the numerical interaction with all compressor simulation behavior as boundary conditions.

Figure 7 shows both instantaneous velocity profiles where expected phenomena are verified. In geometry (A) all inlet suction muffler mass flow rate is impinged through first chamber and consequently goes mainly indirectly to the second chamber. On contrary, in geometry (B), inlet suction mass flow rate comes directly through the tube to the suction muffler outlet and only a few percentage of fluid is flowing to the first suction chamber.

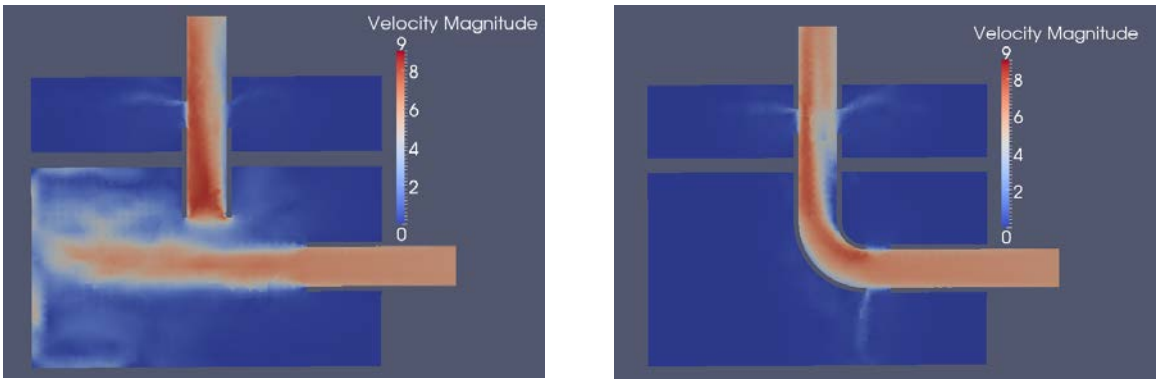

Figure 7. Non-dimensional pressure drop evolution.

Of course pressure drop in suction muffler configuration (B) is going to be lower than the pressure drop in configuration (A), while the pressure pulsation of (B) will be higher than (A). The main question is to know which is the pressure drop reduction to take into account as a balance between noise reduction vs. pressure drop increase for design purposes.

Figure 8 shows the non-dimensional pressure drop sampled by blocks over one compressor cycle, while imposing constant inlet mass flow rate. Despite of not being representative of the compressor operational conditions, the case of constant inlet mass flow rate illustrates very well the significant difference in pressure drop that arises from the two geometries.

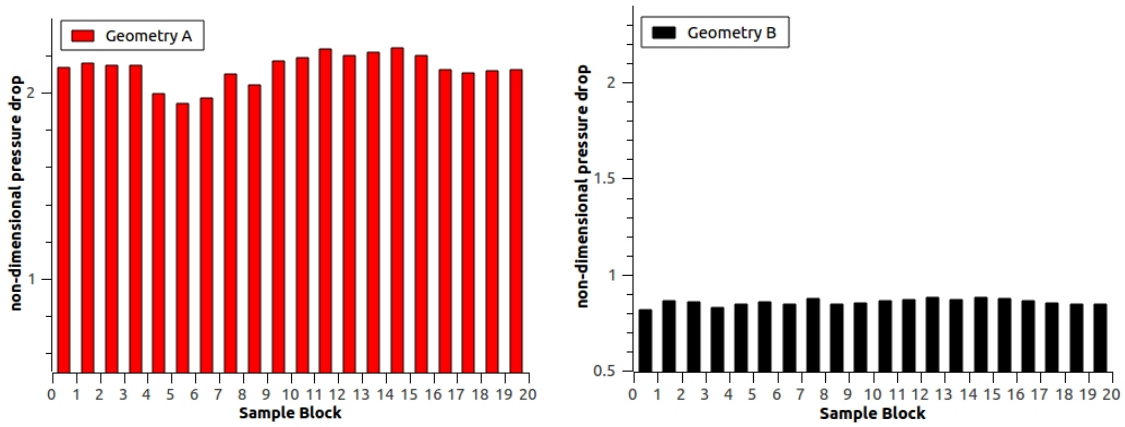

Figure 8. Non-dimensional pressure drop sample by blocks.

Subsequently, the same cases have been simulated, but instead of the inlet mass flow rate, the inlet pressure is imposed. It is reminded that in this approach, the imposed pressure is the p_∞ (the pressure at a distance from the inlet, where the fluid is at rest) and it is given as total pressure (sum of static and dynamic pressure) along with an expansion coefficient. Therefore the static pressure is determined by the velocity. This boundary condition reflects well the real case, where the fluid in the remnant gas chamber is at rest and at nearly constant pressure and the pressure difference across the muffler dictates the flow (allowing also backflows).

The presented results pertain to one compressor cycle, once cyclic behavior is achieved. The cyclic behavior is confirmed graphically, as well as by monitoring the accumulation of mass, whose integral over one cycle should approximate zero.

Figure 9 illustrates the mass flow rate at the outlet of the muffler for the two geometries. As anticipated, the mass flow rate in (B) is higher than in (A). The integration of the curves over the entire period yields 3.38 kg/h for (A) and 4.04kg/h for (B). Figure 9 (right) shows the instantaneous pressure drop over one cycle for the two geometries. As expected, the pressure drop is higher in (A) for most of the cycle**.**

As observed in Figure 9 (left), the curve of the pressure drop across the muffler exhibits lower inertia for the configuration (A), namely, it is more sensitive to the pressure variations at the outlet. This results from the indirectness of configuration (A). The inflow and outflow of (A) are momentarily decoupled. The outflow (either from inlet or outlet orifice) is always initiated by fluid which is at rest in the main chamber, weakly dependent on the inflow conditions. On the other hand, (B) is dictated by one direct flow, so the outflow is strongly dependent on the inflow conditions. Also, the configuration (A) allows higher fluctuation of mass inside the main chamber (as illustrated in Figure 10, which shows the instantaneous mass flow difference between inlet and outlet (Δm) over one period), so the main chamber acts somehow as a buffer between the inflow and the outflow. On the contrary, the main chamber of (B) is quite isolated and does not participate in the flow (Figure 7) – so the mass fluctuation is more limited.

The latter conclusion can also arise by observing Figure 11, which illustrates the inlet and outlet mass flow rate for the two geometries respectively. The two curves are almost identical for configuration (B) while in for (A) the curves are quite distinct when the pressure gradient is high. This implies the indirectness of the configuration (A).

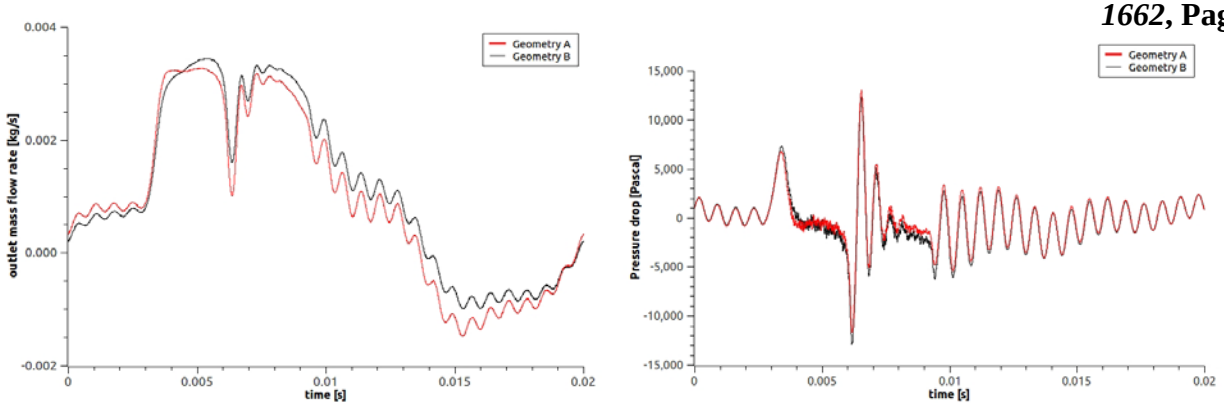

Figure 9. Mass flow rate at the outlet of the muffler for the two configurations (left), and instantaneous pressure drop across the muffler over one cycle (right).

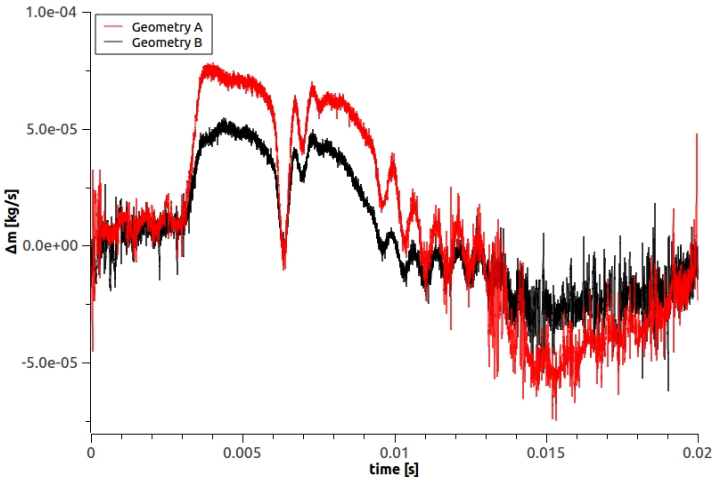

Figure 10. Mass accumulation inside the muffler over one cycle

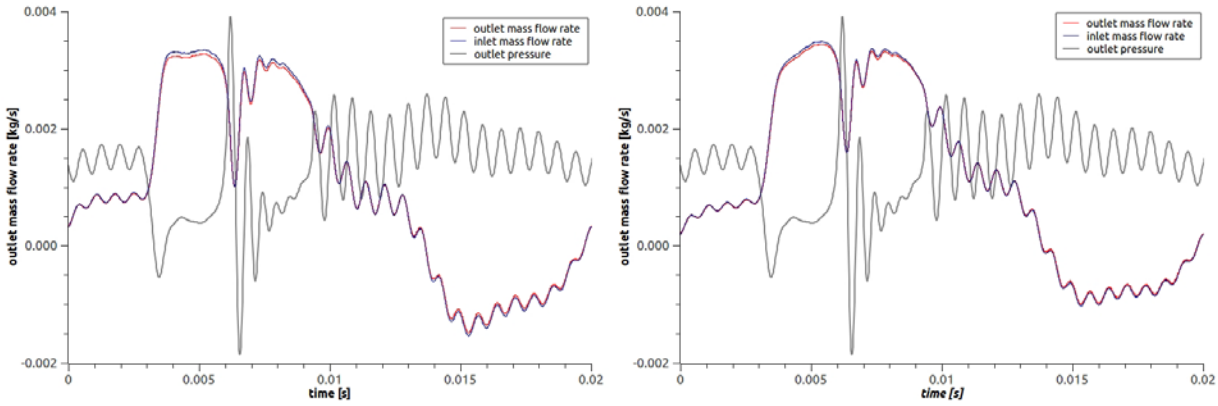

Figure 11. Inlet and outlet mass flow rate, superimposed on the outlet pressure for A (left) and B(right).

6. CONCLUSIONS

A numerical simulation model for compressor suction muffler design is presented based on CFD&HT analysis of suction muffler geometry using as boundary conditions the interaction with numerical simulation tool for the whole compressor analysis. The CFD&HT tool based on LES turbulence models, allowing the use of coarse meshes and high numerical software scalability (improved algorithms) and hardware (High Performance Cluster) shows the real capacity that this kind of tools offer for compressor optimization design. A first academic illustrative case is presented to show the influence of the fluid flow configuration on pressure drop or mass flow rate though geometry.

REFERENCES

Chiva, J., Ventosa, J., Lehmkuhl, O., Pérez-Segarra, C.D., 2011, Modelization of the low Mach Navier-Stokes equations in unstructured meses, *Proceedings of the 7th Int. Conference on Computational Heat and Mass Transfer*.

Choi, J.M., Joo, J.M., Oh, S.K., Park, S.W, 2000, Smart suction muffler design for a reciprocating compressor, *Int. Compressor Engineering Conference at Purdue*.

Damle, R., Rigola, J., Pérez-Segarra, C.D., Castro, J., Oliva, A., 2011, Object oriented simulation of reciprocating compressors: Numerical verification and experimental comparison, *Int. J. Refrig.*, 34: p. 1989-1998.

Pérez-Segarra, C.D., Rigola, J. Oliva, A., 2003, Modelling and numerical simulation of the thermal and fluid dynamic behaviour of hermetic reciprocating compressors. Part I: Theoretical basis, *Int. J. Heating, Ventilating, Air-Conditioning and Refrig. Research*, vol. 9: p. 215-236.

Lehmkuhl, O., Borrell, R., .Pérez-Segarra, C.D., Soria, M., Oliva, A., 2007, A new parallel unstructured CFD code for the simulation of turbulent industrial problems on low cost PC cluster, *Parallel CFD*.

López, J., Lehmkuhl, O. Rigola, J., Pérez-Segarra, C.D., 2012, Use of Low-Mach modelo n a CFD&HT solver for the elements of an object oriented program to numerically simulate hermetic reciprocating compressors, *Int. Compressor Engineering Conference at Purdue*, p. 1385.

Nakano, A, Ninjo, K , 2008, CFD applications for development of hermetic reciprocating compressors, *Int. Compressor Engineering Conference at Purdue*.

Najm, H.N., Wyckoff, P.S., Knio, O.M., 1998, A semi-implicit numerical scheme for reacting flow, *J. of Computational Physiscs*, vol. 143: p. 381-402.

Nicoud F., Ducros, F, 1999, Subgrid-scale stress modeling based on the square of the velocity gradient tensor, *Flow, Turbulence and Combustion*, vol: 62, no. 183: p. 200.

Nicoud, F., 2000, Conservative high-order finite difference schemes for low-mach numbers flows, *J. of Computational Physics*, vol. 158: p. 71-97.

Pereira, E.L.L., Deschamps, C.J., Ribas, F.A., 2000, Performance analysis of reciprocating compressors through computational fluid dynamics, *Int. Compressor Engineering Conference at Purdue*.

Pérez-Segarra, C.D., Escanes, F, Oliva, 1994, A. Numerical study of the thermal and fluid-dynamic behavior of reciprocating compressors, *Int. Compressor Engineering Conference at Purdue*.

Rigola, J., Lehmkuhl, O., Pérez-Segarra, C.D., Oliva, 2012, A. Numerical simulation of the turbulent fluid flow through valves base d on low Mach models; *Int. Compressor Engineering Conference at Purdue*.

Sarioglu, K., Ozdemir, A.R., Orguz, M., Kaya, A., 2012, An experimental and numerical analysis of refrigerant flow inside suction muffler of hermetic reciprocating compressor, *Int. Compressor Engineering Conference at Purdue*.

Singh, R. Soedel, W., 1974, A review of compressor lines pulsation analysis and muffler design research – Part II: Analysis of pulsating flows, *Int. Compressor Engineering Conference at Purdue*.

Verstappen, R., Veldman A.E.P., 2003, Symmetry-preserving discretization of turbulent flow, *J. Computational* Physics, vol. 187: p. 343-368.

Yaneko, N.N., 1971, *The method of fractional step*, Springer-Verlag.

Yoshizawa, A. Kobayashi, K. Kobayashi, T. Taniguchi, N., 2000, A non-equilibrium fixed parameter subgrid-scale model obeying the near wall asymptotic constraint, *Physics of Fluids*, vol. 12, no. 9: p. 2338.

ACKNOWLEDGEMENT

The authors acknowledge the collaboration between CTTC-UPC and Termo Fluids, S.L. company (C06550).